

regions over the period 1990–2009 (see RECCAP special issue, Canadell et al., 2013, http://www.biogeosciences.net/special_issue107.html).

Trends and variability in the air–sea CO₂ fluxes simulated by the employed OBGCMs are driven by the increase in atmospheric CO₂ and by variability and change in ocean temperature, circulation, winds, and biology largely governed by climate variability. The air–sea CO₂ flux arising from the increase in atmospheric CO₂ is often referred to as the flux of anthropogenic CO₂, while the remainder, induced by changes in the natural cycling of carbon in the ocean–atmosphere system is called the “natural” CO₂ component (e.g., Gruber et al., 2009). Although this conceptual separation has its limits (McNeill and Matear, 2013), it provides for a powerful way to understand how different forcings affect the net ocean sink.

DGVM results are compared with estimates of the Residual Land Sink and with remote sensing products indicating trends of greening and browning in the northern region. Regional sources and sink trends are attributed to processes based on factorial simulations.

2 Methods

2.1 Dynamic Global Vegetation Models

Following the studies of Le Quéré et al. (2009) and Sitch et al. (2008), a consortium of Dynamic Global Vegetation Model (DGVM) groups set up a project to investigate further the spatial trends in land–atmosphere flux and agreed to perform a factorial set of DGVM simulations over the historical period, 1901–2009. These simulations have contributed to the RECCAP activity (Canadell et al., 2011, 2013). There are now a variety of DGVMs with origins in different research communities that typically contain alternative parameterisations and a diverse inclusion of processes (Prentice et al., 2007; Piao et al., 2013). DGVMs have emerged from the Land Surface Modelling (LSM), forest ecology, global biogeography, and global biogeochemical modelling communities.

20119

Representative of these research strands are the nine following Dynamic Global Vegetation Models, which are applied here: Hyland (Levy et al., 2004), JULES (Cox, 2001; Clark et al., 2011), LPJ (Sitch et al., 2003), LPJ-GUESS (Smith et al., 2001), NCAR-CLM4 (Thornton et al., 2007, 2009; Bonan and Levis, 2010; Lawrence et al., 2011), ORCHIDEE (Krinner et al., 2005), OCN (Zaehle and Friend, 2010), SDGVM (Woodward et al., 1995; Woodward and Lomas, 2004), VEGAS (Zeng, 2003; Zeng et al., 2005). In this study we focus on two aspects of land surface modelling: the carbon and the hydrological cycle. In the case of land-surface models coupled to GCMs, energy exchange between the land surface and atmosphere is also simulated.

2.2 Ocean carbon-cycle models

A total of four different groups have conducted the factorial simulations over the analysis period with three-dimensional OBGCMs and submitted their results to the RECCAP archive. These are MICOM-HAMOCCv1 (BER) (Assmann et al., 2010), CCSM-WHOI using CCSM3.1 (BEC) (Doney et al., 2009a, b), CCSM-ETH using CCSM3.0 (ETH) (Graven et al., 2012), and NEMO-PlankTOM5 (UEA) (Buitenhuis et al., 2010). Details of the models are given in the Appendix of Wanninkhof et al. (2012). Not all model simulations are independent of each other, as several of them share components. BEC and ETH employ the same BOGCM, but differ in their spinup and surface forcing. The employed models have relatively similar horizontal resolution of the order of 1° to 3° in longitude and latitude, i.e., none of them is eddy-permitting or eddy-resolving. The four ecosystem/biogeochemical models are also of comparable complexity, i.e., including explicit descriptions for at least one phytoplankton and zooplankton group, with some models considering up to three explicitly modeled groups for phytoplankton and two for zooplankton. All models use the same gas exchange parameterization of Wanninkhof (1992), although with different parameters. In particular, the ETH model used a lower coefficient than originally proposed, yielding a global mean gas transfer velocity that is more than 25% lower than those of the other models (Graven et al., 2012). This reduction reflects the mounting evidence based on radiocarbon analyses that the orig-

20120

2.4.2 Ocean

The ocean models have employed two different strategies for creating the initial conditions for the experiments. The first strategy, followed by CCSM-ETH, CCSM-WHOI and BER, involved first a several century long spinup with climatological forcing and with atmospheric CO₂ held constant at its pre-industrial value, bringing these models very close to a climatological steady-state for preindustrial conditions (in some models ~ 1750; in others ~ 1850). In the second step, the models are then integrated forward in time through the historical period until 1948, with atmospheric CO₂ prescribed to follow the observed trend and a climatological forcing. The length of the spinup varies between a few hundred years to several thousand years, resulting in differing global integrated drift fluxes, although their magnitudes are substantially smaller than 0.05 PgCyr⁻¹ with essentially no rate of change. The second strategy, followed by the University of East Anglia, was to initialize the model with reconstructed initial conditions in 1920, and then also run it forward in time until 1948 with prescribed atmospheric CO₂, repeating the daily forcing conditions of a single year (1980). The modelled export production was tuned to obtain an ocean CO₂ sink of 2.2 PgCyr⁻¹ in the 1990s. This second method offers the advantage that the model's carbon fields remain closer to the observations compared to the long spinup approach, but it comes at the cost of generating a drift that affects the mean conditions and to a lesser extent the trend. Tests with the model runs of Le Quéré et al. (2010) suggests the drift in the mean CO₂ sink is about 0.5 PgCyr⁻¹ and the drift in the trend is about 0.005 PgCyr⁻² globally, and is largest in the Southern Ocean. In these runs, both S_O1 and S_O2 are affected by the same drift, and their differences thus removes the drift. From ~ 1950 onward, the models performed two separate simulations:

S_O1: CO₂ only, i.e., atmospheric CO₂ increases, but models are forced with climatological atmospheric boundary conditions (referred to as ACO2 in the RECCAP archive).

20123

S_O2: CO₂ and climate, i.e., as S_O1, but models are forced with “realistic” year-to-year variability in atmospheric boundary conditions (ANTH).

The CCSM-based models performed an additional experiment to better separate between the fluxes of natural and anthropogenic CO₂:

S_O3: pre-industrial and climate, i.e., atmospheric CO₂ is fixed at its pre-industrial level, but atmospheric boundary conditions vary as in S_O2 (PIND).

From these simulations, only the results from 1990 through 2009 were analysed. Only the UEA and CCSM-WHOI models made available results for the S_O1 and S_O2 simulations for the entire analysis time. The results for the BER model for 2009 are incomplete and the CCSM-ETH simulations extend only to 2007. In order to maintain a sufficiently large set of models, we decided to focus our analysis primarily on the 1990 through 2004 period, but include occasionally also the results through 2009, with the important caveat that the latter are based only on two models.

2.5 Output variables

2.5.1 Land

Output variables include those associated with the carbon, hydrological and energy balance over the period 1901–2009. Variables were considered either “Level 1”, and essential, or “Level 2”, desirable, for additional analysis/studies. Output variables were typically at either the monthly or annual resolution, and at the spatial resolution of the individual model application. In this study we analyse a sub-set of the DGVM output, and primarily focus on the carbon cycle variables, Net Primary Productivity (NPP), Heterotrophic Respiration (RH), and the Net Biome Productivity (NBP), and Leaf Area Index (LAI), a measure of vegetation greenness. The land to atmosphere net CO₂ flux is equal in magnitude to the NBP but has the opposite sign, i.e. we adopt the sign convention where a negative value for the net CO₂ flux represents a carbon sink. Here

20124

DGVMs simulate an ensemble mean global RH of $57.5 \pm 9.8 \text{ PgCyr}^{-1}$ over the period 1990 and 2009 (Table 2). All DGVMs simulate an increase in RH for S2 (CO₂ and climate), with an ensemble mean trend of $0.16 \pm 0.05 \text{ PgCyr}^{-2}$ ($P = 0.00$) over the period 1990 to 2009 (Table 2). This is lower than the trend in global NPP, thus explaining the trend towards increasing net land carbon uptake. This is unsurprising as there is a lagged response in increases in RH relative to NPP, reflecting the turnover time of the newly incorporated plant material. The ensemble mean trend in RH is $0.12 \pm 0.06 \text{ PgCyr}^{-2}$ ($P = 0.00$) and $0.04 \pm 0.02 \text{ PgCyr}^{-2}$ ($P = 0.09$) over the same period for the S1 (CO₂ only) and S_L2-S_L1 (the climate effect), respectively (Tables A2, A3), implying the dominant effect on RH is increased substrate for microbial respiration, with the additional litter input into soils, as a consequence of enhanced NPP, rather than enhanced rates of microbial decomposition with rising temperatures. Nevertheless, the simulated mean residence time (MRT = Soil Carbon/RH) of soil organic matter decreases, in response to warming, which is especially pronounced in high latitude regions (Fig. A3). The differences in land-atmosphere flux trends for the CN models, OCN (-0.02 PgCyr^{-2}) and CLM4CN (-0.05 PgCyr^{-2}) are largely due their differences in RH trends at 0.14 and 0.11 PgCyr^{-2} , respectively, rather than differential responses of simulated NPP to elevated CO₂ (Table 2).

Only 4 DGVMs provided wildfire fluxes (CLM4CN, LPJ, LPJ-GUESS, SDGVM). No significant trends in the global wildfire flux were reported by any of the DGVMs. Only two DGVMs (CLM4CN and LPJ) simulated small significant trends of opposite sign in the wildfire flux to the 90 % confidence interval for S_L1 (CO₂ only), possibly reflecting the counteracting effects of CO₂ on plant water use, leading to more moist land surface (reduced flammability), and elevated productivity (increased fuel loads).

3.1.2 Ocean

The global ocean is simulated to have acted as a very substantial sink for atmospheric CO₂, but one that has increased only slightly over the last two decades (see also

20129

discussion in Wanninkhof et al., 2013). The mean ocean sink in the 4 models (CCSM-ETH, CCSM-WHOI, UEA and BER), increased from $\sim -2.0 \text{ PgCyr}^{-1}$ in the early 1990s to $\sim -2.1 \text{ PgCyr}^{-1}$ during the first five years of the 21st century (Fig. 4). The overall sink is largely a consequence of the increase in atmospheric CO₂ (i.e., it corresponds mostly to the uptake flux of anthropogenic CO₂), but it includes a substantial perturbation flux stemming from the impact of climate variability and change on the ocean carbon cycle.

This is confirmed if we separate the mean and variable components by using our factorial experiments, i.e., by using S_O1 results to identify the ocean uptake in the absence of climate variability and change, and the difference between S_O2 and S_O1 as measure of the impact of climate change. This separation reveals that in the absence of climate variability and change, the global ocean uptake would have increased from about $-1.98 \pm 0.04 \text{ PgCyr}^{-1}$ for the 1990–1994 period to $-2.3 \pm 0.09 \text{ PgCyr}^{-1}$ for 2000–2004 (for the two models CCSM-WHOI and UEA that provided S_O1 results up to 2009, the uptake flux would have increased from -1.99 PgCyr^{-1} to -2.56 PgCyr^{-1} for 2005–2009). This global net uptake flux and its substantial trend in time (-0.03 PgCyr^{-2} for 1990–2004, and -0.04 PgCyr^{-2} for 1990–2010) is entirely driven by the increase of atmospheric CO₂ and is – integrated globally – numerically equivalent to the ocean uptake flux of anthropogenic CO₂. Climate variability and change modified these fluxes, and particularly the trend in these models. The four models suggest an enhancement of the uptake in the early 1990s (1990–1994) of about -0.2 PgCyr^{-1} , turning into a reduction of the uptake in the subsequent period (1995–1999), followed by a further reduction in the 2000–2004 period of $\sim +0.1 \text{ PgCyr}^{-1}$. This trend toward reduced uptake in response to climate variability and change of $+0.03 \text{ PgCyr}^{-2}$ nearly completely compensates for the anthropogenic CO₂ driven increase in uptake, causing the overall uptake of CO₂ to have a nearly flat trend over the 1990 through 2004 period of $< 0.01 \text{ PgCyr}^{-2}$. The same tendencies are found for the two models that extend over the entire 1990 through 2009 period: climate change and variability reduces in these models the CO₂ driven trend of -0.04 PgCyr^{-2} by more than $+0.02 \text{ PgCyr}^{-2}$, to around -0.02 PgCyr^{-2} .

20130

Consideration of the different factors affecting the ocean carbon sink following our Taylor expansion, we find increasing sea-surface temperature to be globally one of the most important drivers for the positive trends (reduced sinks) induced by climate change and variability. Over the 1990 through 2004 period, the surface ocean warmed, on average, by $0.004\text{ }^{\circ}\text{C yr}^{-1}$ ($0.005\text{ }^{\circ}\text{C yr}^{-1}$ from 1990 through 2009). Isochemically, this leads to an increase of the oceanic $p\text{CO}_2$ of $\sim 0.06\text{ }\mu\text{atm yr}^{-1}$, which appears small. However, it needs to be compared with the trend in the global mean air–sea $p\text{CO}_2$ difference of about $\sim 0.1\text{ }\mu\text{atm yr}^{-1}$ that is required in order to generate a trend in the ocean uptake of -0.03 PgCyr^{-2} (see e.g., Matsumoto and Gruber, 2005; Sarmiento and Gruber, 2006).

3.2 Regional trends

3.2.1 Land

Spatial correlations between trends in drivers and carbon fluxes (NBP, NPP, RH) were significant for precipitation (0.36, 0.5, 0.48 respectively; $P < 0.05$), but not for temperature (see Table A11), underlining the sensitivity of carbon cycle models to precipitation changes at the multi-year to decadal timescale.

3.2.2 Northern land

All DGVMs agree on a land C sink over the northern land region, with a mean land–atmosphere flux of $-1.03 \pm 0.30\text{ PgCyr}^{-1}$, over the period 1990–2009 (Fig. A4, Table 2). The ensemble mean land–atmosphere flux trend is near zero for this region between 1990 and 2009 (Fig. A5). Although 4 of 9 DGVMs simulate reductions in the land sink over the northern land region, none of the trends from the 9 DGVMs are significant at the 95 % confidence level (Table 2). Of particular interest are sub-regions with a simulated positive land–atmosphere flux trend (Fig. 5), implying a diminishing sink of atmospheric CO_2 , or an increasing source of CO_2 to the atmosphere. At least 6 mod-

20131

els out of 9 agree on a decreasing regional land sink across some areas in Temperate North America, Eastern Europe, North-East China and Mongolia (Fig. 5). These net flux trends largely correspond to regions with negative trends in precipitation (Fig. 6).

Over the northern region, DGVMs simulate an ensemble mean NPP of $24.1 \pm 4.48\text{ PgCyr}^{-1}$, which represents almost 40 % of the global total (Table 2). All DGVMs simulate an increase in northern NPP over this period, with a trend in NPP of $0.06 \pm 0.02\text{ PgCyr}^{-2}$ ($P = 0.00$) (Table 2). However, enhanced productivity in the northern land region accounts for only around 29 % of the simulated global trend in NPP. The ensemble mean NPP trend of $0.06 \pm 0.02\text{ PgCyr}^{-2}$ ($P = 0.00$) from simulation S2 (CO_2 and climate forcing) compares to a trend of $0.07 \pm 0.03\text{ PgCyr}^{-2}$ ($P = 0.00$), and $-0.00 \pm 0.04\text{ PgCyr}^{-2}$ ($P = 0.85$) for the S1 (CO_2 only) and S2–S1 (the climate effect), respectively (Tables A2, A3). All DGVMs simulate a positive trend in NPP in response to elevated CO_2 across the northern land region and trends are all significant to the 95 % confidence level with the exception of CLM4CN ($P = 0.21$). Large areas in Temperate North America and Asia have experienced warming combined with reductions in precipitation over the period 1990–2009 (Fig. 5).

The ensemble mean NPP for North America, Europe and North Asia are $7.78 \pm 1.38\text{ PgCyr}^{-1}$, $5.08 \pm 1.40\text{ PgCyr}^{-1}$, and $11.20 \pm 1.99\text{ PgCyr}^{-1}$, respectively (Table A5). Despite the two-fold difference in mean NPP, NPP trends for North America, Europe and North Asia are similar, at $0.021 \pm 0.008\text{ PgCyr}^{-2}$ ($P = 0.02$), $0.018 \pm 0.006\text{ PgCyr}^{-2}$ ($P = 0.00$) and $0.024 \pm 0.015\text{ PgCyr}^{-2}$ ($P = 0.01$), respectively (Table A5). DGVMs simulate larger mean NPP in Temperate compared to Boreal regions with mean NPP in Temperate North America and Asia of $4.22 \pm 0.83\text{ PgCyr}^{-1}$ and $7.09 \pm 1.03\text{ PgCyr}^{-1}$, respectively, compared to $3.57 \pm 1.21\text{ PgCyr}^{-1}$ and $4.12 \pm 1.46\text{ PgCyr}^{-1}$ in Boreal North America and Asia, respectively (Table A5). DGVMs simulate a significant positive trend in Boreal North America and Boreal Asia of $0.014 \pm 0.007\text{ PgCyr}^{-2}$ ($P = 0.02$) and $0.018 \pm 0.006\text{ PgCyr}^{-2}$ ($P = 0.01$), respectively. DGVM NPP trends in both Temperate North America and Asia are smaller than those for Boreal regions but are not significant at the 95 % confidence level (Table A5).

20132

3.2.5 Qualitative change in processes

A qualitative assessment of the differential responses of the underlying land processes to changes in environmental conditions, and their contribution to the sink-source land-atmosphere flux trends are shown in Fig. 8. Many regions are simulated to have a negative land-atmosphere flux trend, with increases in NPP leading increases in RH. However the locations with positive trends over the period 1990 to 2009, i.e. the red colours in Fig. 8, generally fall into two categories: First, regions where models simulate a positive trend in NPP, but an even larger positive trend in RH (eastern Europe, South East USA, Amazonia, South China, North America Tundra). Warming is likely to enhance both NPP and RH in high latitude ecosystems, but primarily RH in low latitudes. Reduced precipitation may partially or fully offset the benefits of elevated atmospheric CO₂ abundance on NPP, and the response of RH to changes in precipitation is not obvious, as this depends on the initial soil moisture status. This is because microbial activity increases with increasing soil moisture at low moisture levels, before reaching a maximum activity, and then begins to decline as water fills the soil pore spaces and oxygen becomes more limiting to respiration. Locations in eastern USA, southern Asia, northern boreal China, south-eastern South America, western and southern Australia are simulated to have negative NPP trends over the last two decades, as a result of reduced rainfall, and there is a less negative trend in RH, possibly due to a reduction in microbial respiration rates with increased soil dryness. The warming and drying in Inner Asia (North East China and Mongolia) and southern Australia is simulated to reduce the rate of microbial decomposition in these regions (Fig. A3), which partly opposes the NPP-driven lagged decrease of RH. The source trend in eastern Europe is simulated as a combination of a negative trend in NPP, as a result of a combination of elevated temperatures and reduced precipitation (i.e. soil drying), and a positive trend in RH, despite reduced plant litter input.

20137

3.2.6 Ocean

3.2.7 Regional fluxes

The large-scale distribution of the modeled mean surface fluxes consists of strong outgassing in the tropical regions, especially in the Pacific, and broad regions of uptake in the mid latitudes, with a few regions in the high latitudes of particularly high uptake, such as the North Atlantic (Fig. 9). This pattern is largely the result of the exchange flux of natural CO₂ that balances globally to a near zero flux, but exhibits regionally strong variations (Gruber et al., 2009). Superimposed on this natural CO₂ flux pattern is the uptake of anthropogenic CO₂, which leads to uptake everywhere, but with substantial regional differences. Large anthropogenic CO₂ uptake fluxes occur in the regions of surface ocean divergence, such as the equatorial Pacific and particularly the Southern Ocean (Sarmiento et al., 1992; Mikaloff Fletcher et al., 2006). This is a result of the divergence causing waters to come from below to the surface which have not been exposed to the atmosphere for while, thereby permitting them to take up a substantial amount of anthropogenic CO₂. This reduces the outgassing that typically characterizes these regions as a result of these upwelling waters bringing with them also high carbon loads from the remineralization of organic matter.

Over the analysis period, the air–sea CO₂ fluxes exhibit only a remarkably small trend in most places with some regions increasing in uptake, while others show a positive flux anomaly, i.e., lesser uptake. Thus the small global trend in ocean uptake over the 1990 through 2004 analysis period is a result of also the individual regions having relatively modest trends.

3.2.8 Process-decomposition

The regional flux trends are, however, much smaller than expected from an ocean with constant circulation that is only responding to increasing atmospheric CO₂ and hence would tend to increase its uptake of anthropogenic CO₂ through time (Fig. 10). In the

20138

absence of climate variability and change, all regions would have flux density trends of more than $-0.05 \text{ g C m}^{-2} \text{ yr}^{-2}$, with some regions, such as the Southern Ocean exceeding $-0.15 \text{ g C m}^{-2} \text{ yr}^{-2}$. But climate variability and change compensate these negative trends in every single region by increasing them by $+0.04 \text{ g C m}^{-2} \text{ yr}^{-2}$ or more (with the exception of the South Pacific), such that the overall trends fluctuate from region to region around zero (Fig. 10). The largest reductions in trends are simulated to occur in the North and Equatorial Pacific and in the North Atlantic, where they even cause a change in the sign of the overall trend. A similar, although slightly more moderate pattern is seen if the analysis is undertaken for the entire 1990 through 2009 period on the basis of two models only. The most important difference is found in the North Atlantic, where the climate variability impact is substantially smaller, and not offsetting the anthropogenic CO_2 trend when analyzed for 1990–2009.

The mechanisms driving the oceanic flux trends differ between the analyzed regions. In some regions, surface ocean warming dominates and hence reduces or even cancels increasing ocean anthropogenic CO_2 uptake, as is the case globally (Roy et al., 2011). In other regions, wind changes dominate and yet in other regions, flux trends reflect changes in DIC and Alk, possibly a result of changes in ocean circulation, mixing, and biological productivity.

4 Discussion

4.1 Land

DGVMs simulate an increase in land carbon uptake over the period 1990–2009. The result agrees with earlier findings of Sarmiento et al. (2010), who suggested a large increase in the RLS between the periods 1960–1988 and 1989–2009 (Table A9). The ensemble mean land-atmosphere flux increased by $-1.11 \text{ Pg C yr}^{-1}$ for the same period, compared to the estimated RLS increase of $-0.88 \text{ Pg C yr}^{-1}$ from Sarmiento et al. (2010). The DGVM ensemble trends in land uptake for the globe,

20139

northern, tropical and southern land regions of -0.06 ± 0.03 , 0.00 ± 0.01 , -0.04 ± 0.01 , $-0.02 \pm 0.02 \text{ Pg C yr}^{-2}$, respectively, compare favorably with the inversion estimates of -0.06 ± 0.04 , -0.01 ± 0.01 , -0.04 ± 0.02 , $-0.01 \pm 0.01 \text{ Pg C yr}^{-2}$, over the period, 1990–2009. Although encouraging, these results should be interpreted with caution because the inversion accounts for any trend in the land use change flux over this period, whereas DGVMs had fixed land use. For this reason we do not compare results at scales finer than the zonal one.

There is empirical evidence for a large increase in biomass in intact forest in the tropical South America and Africa (Pan et al., 2011; Baker et al., 2004; Lewis et al., 2009a, b), which is consistent with the DGVM projections presented here. Subsequently, Lewis et al. (2009b) found broad agreement between biomass trends from observations and from a suite of carbon cycle models applied with 20th century forcing of climate and atmospheric CO_2 content, using a similar protocol to the current analysis. This suggests a large possible role of CO_2 fertilization in stimulating plant productivity in tropical ecosystems. DGVMs suggest a large component of the uptake trend is associated with a positive NPP response to elevated CO_2 , which is broadly consistent with the enhancement of forest production due to CO_2 observed in Free Air Carbon Enrichment (FACE) experiments (Norby et al., 2005), albeit they are largely located in temperate forest ecosystems. However, recent studies have highlighted the role of nitrogen in limiting the long term CO_2 response (Canadell et al., 2007; Norby et al., 2010) in these ecosystems. The long-term plant response to elevated CO_2 is likely affected by nutrients and its impact on plant C allocation (Zaehle et al., 2014), however only two out of the nine models used here (CLM4CN and OCN) include interactive nutrient cycling (see DGVM characteristics, Table A1).

In contrast to the large trend in net C uptake across the tropics, DGVMs simulate no statistically significant trend over the northern land. In particular, trends in NPP over Temperate regions are smaller than those in Boreal regions, and are also not significant. Many temperate areas have experienced a decrease in rainfall between 1990 and 2009, and suffered periods of prolonged and severe drought. Examples include

20140

the drought in western USA 2000–2004 (McDowell et al., 2008; Anderreg et al., 2012), and the 2003 summer heatwave in Europe (Ciais et al., 2005). These are likely to have had a detrimental effect on the land C uptake (Ciais et al., 2005). This is particularly relevant as climate models agree on a future warming and reduced summer precipitation over continental mid-latitudes (IPCC, 2007).

5 Modelling ecosystem structure and function in water stressed environments remains a challenge for DGVMs (Morales et al., 2005; Keenan et al., 2009). In general, there is a need for a greater understanding of the mechanisms behind drought-induced plant mortality (Allen et al., 2010; McDowell et al., 2011), and changes in plant water use
10 (De Kauwe et al., 2013). Incorporating hydraulic failure under drought stress improved the ability of the LPJ-GUESS model to simulate the distribution and productivity of xeric and arid vegetation types on a global scale (Hickler et al., 2006); however, the latter is not included in most models. In general, an improvement in the description of vegetation is needed with the adoption of more plant trait information now available
15 (Kattge et al., 2011).

Satellite observations suggest a general greening trend in high latitudes with an earlier onset and longer growing season in high latitude ecosystems, which is reproduced by the DGVMs. Observations suggest a greening Tundra and a slower greening and possible browning in some regions of the boreal forest (Tucker et al., 2001; Bhatt et al.,
20 2010), especially in North America (Beck and Goetz, 2011). In tundra ecosystems, an earlier onset is attributed to warming and earlier snowmelt. In these ecosystems radiation melts snow in the early spring, and the start of growing season corresponds to near peak in radiation. Thus any temperature induced early snowmelt (McDonald et al.,
25 2004; Sitch et al., 2007) is likely to enhance plant production. Warming may not have such a great effect on the offset of the growing season in Arctic tundra ecosystems as this may be driven primarily by radiation. DGVMs simulate a significant positive trend in NPP Boreal North America and Boreal Asia and Tundra. Nitrogen limitation is also likely to constrain the carbon cycle at high latitudes. Only 2 out of 9 DGVMs studied

20141

here included a fully interactive carbon and nitrogen cycle, and it was not possible to quantify N-limitations effects on regional trends in this study.

DGVMs simulate decreasing NPP across North East China and Mongolia, contributing to the overall decreasing land uptake trend, in response to recent climate. In a regional study, Poulter et al. (2013) investigated the differential response of cool semi-arid ecosystems to recent warming and drying trends across Mongolia and Northern China, using multiple sources of evidence, including, LPJ DGVM, FPAR remotely sensed data (derived from GIMMS NDVI3g) and tree-ring widths. They found coherent pattern of high-precipitation sensitivity across data sources, which showed some
5 areas with warming-induced springtime greening and drought-induced summertime browning, and limitations to NPP explained mainly by soil moisture.
10

Browning is a consequence of regional drought, wildfire and insect outbreak, and their interaction, especially in North America (Beck and Goetz, 2011). Disturbance plays a key role in the ecology of many global ecosystems. For example, wildfire plays
15 a dominant role in the carbon balance of boreal forest in central Canada and other regions (Bond-Lamberty et al., 2007), and insect outbreaks like the mountain pine beetle epidemic 2000–2006; British Columbia, Canada, resulted in the transition of forests from a small carbon sink to a source (Kurz et al., 2008). In general disturbance and forest management are inadequately represented by the current generation of DGVMs,
20 even though several models include simple prognostic wildfire schemes (Table A1), while some are starting to include other disturbance types such as insect attacks (Jönsson et al., 2012) and windthrow (Lagergren et al., 2012). The improvement of DGVMs to include representations of globally and regionally important disturbance types and their response to changing environmental conditions is a priority.

25 4.2 Ocean

The investigated BOGCMs consistently simulate an ocean characterized by a substantial uptake of CO₂ from the atmosphere, but with a global integrated trend in the two recent decades that is substantially smaller than that expected based on the in-

20142

crease in atmospheric CO₂. Results based on the predictions from ocean inversion and ocean Green function methods (Mikaloff Fletcher et al., 2006; Gruber et al., 2009; Khatiwala et al., 2010) suggest an increase in ocean uptake with a trend of the order of $-0.04 \text{ Pg C yr}^{-2}$ over the analysis period (see also Wanninkhof et al., 2013). These latter methods assume constant circulation, while our simulations here include the impact of climate variability and change.

Our analyses reveal indeed that recent climate variability and change has caused the ocean carbon cycle to take up less CO₂ from the atmosphere than expected on the basis of the increase in atmospheric CO₂, i.e., it reduces the efficiency of the ocean carbon sink. Globally, we demonstrated that this efficiency reduction is primarily a result of ocean warming, while regionally, many more processes (e.g., wind changes, alkalinity/DIC concentrations changes) are at play.

Is this reduction in uptake efficiency over the analysis period the first sign of a positive feedback between global warming and the ocean carbon cycle – or alternatively, could it be due to natural decadal-scale variability in air–sea CO₂ fluxes? Without a formal attribution study, it is not possible to provide a firm answer. We suspect that the majority of the trend in the efficiency is due to “natural” decadal-scale variability, however, largely based on the results of McKinley et al. (2011) and Fay and McKinley (2013) who showed that whereas trends in oceanic $p\text{CO}_2$ (and air–sea CO₂ fluxes) are variable on a decadal time-scale, they converge towards atmospheric $p\text{CO}_2$ trends when analyzed over a longer 30 yr period for most global regions. Nevertheless, they also show that in the permanently-stratified subtropical gyre of the North Atlantic, warming (partly driven by anthropogenic climate change) has started to reduce ocean uptake in recent years. In the Southern Ocean, where Le Quéré et al. (2007) and Lovenduski et al. (2008) used models to suggest a reduction in ocean carbon uptake efficiency over the past 25 yr in response to increasing Southern Ocean winds, Fay and McKinley (2013) concluded that the data are insufficient to draw any conclusions.

We should note that the associated uncertainties remain large. Of particular concern is the moderate success of the models to simulate the time-mean ocean sinks and

20143

their long-term seasonal cycle (e.g. McKinley et al., 2006). Furthermore, some of the models underestimate the oceanic uptake of transient tracers such as anthropogenic radiocarbon (see e.g., Graven et al., 2012). Such a reduction in the oceanic uptake efficiency is also not suggested by independent measures of oceanic CO₂ uptake, such as the atmospheric O₂/N₂ method (Manning and Keeling, 2006; Ishidoya et al., 2012), albeit the large uncertainties in these estimates make the determination of trends in uptake highly uncertain.

4.3 Reducing uncertainty in regional sinks

In order to better quantify the regional carbon cycle and its trends, DGVM and ocean carbon cycle models need to improve both process representations and model evaluation and benchmarking (Luo et al., 2012). There is a need for up to date global climate and land use and cover change datasets to force the DGVMs, as well as a deeper investigation of the quality and differences between the different reanalysis products used to force ocean carbon cycle models. Also techniques such as detection and attribution can be applied to elucidate trends in the regional carbon cycle and their drivers.

4.3.1 Model benchmarking

There is a critical need for comprehensive model benchmarking, as a first step to attempt to reduce model uncertainty. Several prototype carbon cycle benchmarking schemes have been developed (Randerson et al., 2009; Cadule et al., 2010). A more in depth evaluation and community benchmarking set needs to be agreed and implemented, which also evaluates models for their implicit land response timescales (especially relevant in the discussion on future tipping elements and non-linear future responses) and for the simulated carbon, water and nutrient cycles. New emerging frameworks now exist (Blyth et al., 2011; Abramowitz, 2012; Luo et al., 2012; Dalmonch and Zaehle, 2013).

20144

4.3.2 Model resolution

5 Simulated ocean carbon dynamics may be sensitive to horizontal resolution, particularly as model resolution improves sufficiently to adequately capture mesoscale eddies. Mesoscale turbulence influences the ocean carbon cycle in a variety of ways, and the present eddy parameterizations may not adequately capture the full range of effects and the responses to climate variability and change. For example, mesoscale processes are thought to modulate biological productivity by altering the supply of limiting nutrients (Falkowski et al., 1991; McGillicuddy et al., 1998; Gruber et al., 2011). A particularly crucial issue involves the wind-driven overturning circulation in the Southern Ocean, where non-eddy resolving models indicate a strong sensitivity of the overturning circulation and ocean carbon uptake to surface wind stress (Le Quere et al., 2007; Lovenduski et al., 2008). Some eddy-resolving models in contrast suggest that enhanced wind stress is dissipated by increased eddy activity, leading to only a small increase in overturning (Boning et al., 2008), though more recent results indicate a larger response (Gent and Danabasoglu, 2011).

4.3.3 Model structure

20 There is a need for improved representation of ecological processes in land and ocean models, e.g. nutrient cycling (N, P), disturbance (wildfire, wind-throw, insects), land use and land cover change in land models and better representation of the key functional diversity in ocean biogeochemical models. DGVMs need to represent land use and land cover changes, forest management and forest age, to improve estimates of the regional and global land carbon budget. There are recent developments to include nutrient dynamics, mostly nitrogen, into global land biosphere models (as reviewed by Zaehle and Dalmonech, 2011). Too few model simulations are available to date to allow for an ensemble model trend assessment. However, a few general trends appear robust: As evident from Table 2, C–N models generally show less of a response to increasing atmospheric CO₂ due to nitrogen limitation of plant production. N dynam-

20145

ics further alter the climate–carbon relationship, which tend to reduce the C loss from temperate and boreal terrestrial ecosystems due to warming; however, with a considerable degree of uncertainty (Thornton et al., 2009; Sokolov et al., 2008; Zaehle et al., 2010). Changes in the nitrogen cycle due to anthropogenic reactive nitrogen additions (both fertiliser to croplands and N deposition on forests and natural grasslands) further modify the terrestrial net C balance and contribute with -0.2 to -0.5 PgCyr⁻¹ to current land sink, with a geographic distribution closely related to that of anthropogenic reactive nitrogen deposition (Zaehle and Dalmonech, 2011). Zaehle et al. (2011), using the OCN model, have estimated the 1995–2005 trend in land uptake due to N deposition as -1.1 ± 1.7 TgCyr⁻², with strong regional differences, depending on the regional trends in air pollution and reactive N loading of the atmosphere and the nitrogen status of the ecosystems, which are generally lower in less responsive in ecosystems close to nitrogen saturation highly polluted regions.

15 There are several additional land processes that have not been considered in this current multi-model analysis. These include the effects of aerosols and tropospheric ozone on the carbon cycle. Unlike a global forcing agent such as CO₂, the effects of air pollutants (aerosols, NO_x, and O₃) with their shorter atmospheric lifetimes are at the regional scale. Aerosol induced changes in radiation quantity and quality (i.e. the ratio of diffuse to direct) affect plant productivity and the land sink (Mercado et al., 2009). From around 1960 onwards until the 1980s radiation levels declined across industrialized regions, a phenomenon called “global dimming”, followed by a recent brightening in Europe and North America with the adoption of air pollution legislation. Reductions in acid rain have been found to greatly influence trends in riverine DOC, vegetation health, and rates of soil organic matter decomposition. Tropospheric ozone is known to be toxic to plants and lead to reductions in plant productivity, and reduce the efficiency of the land carbon sink (Sitch et al., 2007; Anav et al., 2011). Drivers of the land carbon sink related to air pollution, e.g. N deposition, acid precipitation, diffuse and direct radiation, and surface O₃ have varied markedly in space and time over recent decades.

20146

Similar gaps need to be addressed in ocean biogeochemical models. The ecosystem modules in the current generation of BOGCMs lack the ability to assess many of the suggested mechanisms by which climate and ocean acidification could alter marine biogeochemistry and ocean carbon storage. Proposed biological processes that could influence ocean carbon uptake and release involve, for example, decoupling of carbon and macro-nutrient cycling, changes in micro-nutrient limitation, variations in elemental stoichiometry in organic matter, and changes in the vertical depth-scale for the respiration of sinking organic carbon particles (e.g., Boyd and Doney, 2003; Sarmiento and Gruber, 2006). Some advances have been made with the incorporation of dynamic iron cycling and iron limitation, multiple plankton groups, calcification, and nitrogen fixation (Le Quéré et al., 2005). However, the evaluation of these aspects of the models is currently hindered by both data and process-level information limitations.

4.3.4 Climate and land use and cover datasets

In addition to model structure, the choice of climate forcing and model initial conditions can also contribute to differences between the simulated terrestrial carbon sink. At regional scales, differences in land cover can introduce ~ 10 % uncertainty in simulated regional-scale GPP (Jung et al., 2007; Quaife et al., 2008) and about a 3.5 % uncertainty for global NPP. Climate forcing uncertainty tends to have larger effects on carbon flux uncertainty than land cover (Hicke, 2005; Poulter et al., 2011) with up to 25 % differences in GPP reported over Europe (Jung et al., 2007) and a 10 % difference for global NPP (Poulter et al., 2011). Climate forcing uncertainty and land cover (i.e., PFT distributions) can alter long-term trends in NBP and inter-annual variability of carbon fluxes to climate (Poulter et al., 2011). The DGVMs applied here did not consider LULCC. This is an active area of research; models need a consistent implementation of LULCC. Uncertainties in the simulated net land use flux are associated with assumptions on the implementation of LULCC gridded maps (e.g. whether conversion to cropland in a grid-cell is taken preferentially from grassland, forest, or from both), simulated biomass estimates, and subsequent decomposition rates. However DGVMs

20147

offer the exciting prospect to disentangle the component fluxes associated with land use (e.g. direct emissions, and legacy fluxes), and to separate the environmental and direct human impacts on the net LU flux.

5 Conclusions

Land models suggest an increase in the global land net C uptake over the period 1990–2009, mainly driven by trends in NPP, in response to changes in climate and atmospheric CO₂ concentration. Over the same period, ocean models suggest a negligible increase in net ocean C uptake; a result of ocean warming counteracting the expected increase in ocean uptake driven by the increase in atmospheric CO₂. At the sub-regional level, trends vary both in sign and magnitude, particularly over land. Areas in Temperate North America, eastern Europe, North-East China, show a decreasing regional land sink trend, due to regional drying, suggesting a possibility for a transition to a net carbon source in the future if drying continues or drought become more severe and/or frequent. In the ocean, the trends tend to be more homogeneous, but the underlying dynamics differ greatly, ranging from ocean warming, to winds, and to changes in circulation/mixing and ocean productivity, making simple extrapolations into the future difficult.

Our conclusions need to be viewed with several important caveats: Few land models include a prognostic representation of wildfire and no land model represents other disturbances and their interactions, indicating the model response to warming and drought may be conservative in some regions. In addition, only a few models include a fully coupled carbon–nitrogen cycle. Ocean models tend to be too coarse in resolution to properly represent important scales of motions and mixing, such as eddies and other mesoscale processes, and coastal boundary processes. Furthermore, their representation of ocean ecosystem processes and their sensitivity to climate change and other stressors (e.g. ocean acidification, deoxygenation, etc.; Gruber, 2011; Boyd, 2011) is rather simplistic.

20148

- Ballantyne, A. P., Alden, C. B., Miller, J. B., Tans, P. P., and White, J. W. C.: Increase in observed net carbon dioxide uptake by land and oceans during the past 50 years, *Nature*, 488, 70–72, doi:10.1038/nature11299, 2012.
- Battle, M., Bender, M. L., Tans, P. P., White, J. W. C., Ellis, J. T., Conway, T., and Francey, R. J.: Global carbon sinks and their variability inferred from atmospheric O₂ and δ¹³C, *Science*, 287, 2467–2469, 2000.
- Beaulieu, C., Sarmiento, J. L., Mikaloff Fletcher, S. E., Chen, J., and Medvigy, D.: Identification and characterization of abrupt changes in the land uptake of carbon, *Global Biogeochem. Cy.*, 26, GB1007, doi:10.1029/2010GB004024, 2012.
- Beck, S. A. and Goetz, S. J.: Satellite observations of high northern latitude vegetation productivity changes between 1982 and 2008: ecological variability and regional differences, *Environ. Res. Lett.*, 6, 045501, doi:10.1088/1748-9326/6/4/045501, 2011.
- Bhatt, U. S., Walker, D. A., Reynolds, M. K., Comiso, J. C., Epstein, H. E., Jia, G., Gens, R., and Pinzon, J. E., Tucker, C. J., Tweedie, C. E., and Webber, P. J.: Circumpolar Arctic tundra vegetation change is linked to sea ice decline, *Earth Interact.*, 14, 1–20, 2010.
- Buermann, W., Lintner, B. R., Koven, C. D., Angert, A., Pinzon, J. E., Tucker, C. J., and Fung, I. Y.: The changing carbon cycle at Mauna Loa observatory, *P. Natl. Acad. Sci. USA*, 104, 4249–4254, 2007.
- Blyth, E., Clark, D. B., Ellis, R., Huntingford, C., Los, S., Pryor, M., Best, M., and Sitch, S.: A comprehensive set of benchmark tests for a land surface model of simultaneous fluxes of water and carbon at both the global and seasonal scale, *Geosci. Model Dev.*, 4, 255–269, doi:10.5194/gmd-4-255-2011, 2011.
- Bonan, G. B. and Levis, S.: Quantifying carbon-nitrogen feedbacks in the Community Land Model (CLM4), *Geophys. Res. Lett.*, 37, L07401, doi:10.1029/2010GL042430, 2010.
- Böning, C. W., Disper, A., Visbeck, M., Rintoul, S. R., and Schwarzkopf, F. U.: The response of the Antarctic Circumpolar Current to recent climate change, *Nat. Geosci.*, 1, 864–869, 2008.
- Bousquet, P., Peylin, P., Ciais, P., Friedlingstein, P., Lequere, C., and Tans, P.: Interannual CO₂ sources and sinks as deduced by inversion of atmospheric CO₂ data, *Science*, 290, 1342–1346, 2000.
- Boyd, P. W.: Beyond ocean acidification, *Nat. Geosci.*, 4, 273–274, 2011.
- Boyd, P. and Doney, S. C.: The impact of climate change and feedback process on the ocean carbon cycle, in: *Ocean Biogeochemistry*, edited by: Fasham, M., Springer, 157–193, 2003.

20151

- Broecker, W. S., Peng, T.-H., Ostlund, G., and Stuiver, M.: The distribution of bomb radiocarbon in the ocean, *J. Geophys. Res.*, 90, 6953–6970, 1985.
- Buitenhuis, E. T., Rivkin, R. B., Sailley, S., and Le Quéré, C.: Biogeochemical fluxes through microzooplankton, *Global Biogeochem. Cy.*, 24, GB4015, doi:10.1029/2009GB003601, 2010.
- Cadule, P., Friedlingstein, P., Bopp, L., Sitch, S., Jones, C. D., Ciais, P., Piao, S. L., and Peylin, P.: Benchmarking coupled climate-carbon models against long-term atmospheric CO₂ measurements, *Global Biogeochem. Cy.*, 24, GB2016, doi:10.1029/2009GB003556, 2010.
- Canadell, J.: Saturation of the Terrestrial Carbon Sink, 2007.
- Canadell, J. G., Pataki, D., Gifford, R., Houghton, R. A., Lou, Y., Raupach, M. R., Smith, P., and Steffen, W.: Saturation of the terrestrial carbon sink, in: *Terrestrial Ecosystems in a Changing World*, edited by: Canadell, J. G., Pataki, D., and Pitelka, L., The IGBP Series, Springer-Verlag, Berlin Heidelberg, 59–78, 2007.
- Canadell, J. G., Ciais, P., Gurney, K., Le Quéré C., Piao, S., Raupach, M. R., and Sabine, C. L.: An international effort to quantify regional carbon fluxes, *EOS*, 92, 81–82, 2011.
- Canadell, J. G., Ciais, P., Sabine, C., and Joos, F. (Eds.): REgional Carbon Cycle Assessment and Processes (RECCAP), Special Issue, *Biogeosciences*, http://www.biogeosciences.net/special_issue107.html, 2013.
- Chevallier, F., Ciais, P., Conway, T. J., Aalto, T., Anderson, B. E., Bousquet, P., Brunke, E. G., Ciattaglia, L., Esaki, Y., Frölich, M., Gomez, A., Gomez-Pelaez, A. J., Haszpra, L., Krummel, P. B., Langenfelds, R. L., Leuenberger, M., Machida, T., Maignan, F., Matsueda, H., Morguí, J. A., Mukai, H., Nakazawa, T., Peylin, P., Ramonet, M., Rivier, L., Sawa, Y., Schmidt, M., Steele, L. P., Vay, S. A., Vermeulen, A. T., Wofsy, S., and Worthy, D.: CO₂ surface fluxes at grid point scale estimated from a global 21-year reanalysis of atmospheric measurements, *J. Geophys. Res.*, 115, D21307, doi:10.1029/2010JD013887, 2010.
- Ciais, P., Tans, P. P., Trolier, M., White, J. W. C., and Francey, R. J.: A large Northern Hemisphere terrestrial CO₂ sink indicated by the ¹³C/¹²C ratio of atmospheric CO₂, *Science*, 269, 1098–1102, doi:10.1126/science.269.5227.1098, 1995.
- Clark, D. B., Mercado, L. M., Sitch, S., Jones, C. D., Gedney, N., Best, M. J., Pryor, M., Rooney, G. G., Essery, R. L. H., Blyth, E., Boucher, O., Harding, R. J., Huntingford, C., and Cox, P. M.: The Joint UK Land Environment Simulator (JULES), model description – Part 2: Carbon fluxes and vegetation dynamics, *Geosci. Model Dev.*, 4, 701–722, doi:10.5194/gmd-4-701-2011, 2011.

20152

- Conway, T. J., Lang, P. M., and Masarie, K. A.: Atmospheric Carbon Dioxide Dry Air Mole Fractions from the NOAA ESRL Carbon Cycle Cooperative Global Air Sampling Network, 1968–2010, Version: 2011-06-21, available at: <ftp://ftp.cmdl.noaa.gov/ccg/co2/flask/event/>, 2011.
- 5 Cox, P. M.: Description of the “TRIFFID” dynamic global vegetation model, Hadley Centre, Technical Note 24, 2001.
- Dalmonech, D. and Zaehle, S.: Towards a more objective evaluation of modelled land-carbon trends using atmospheric CO₂ and satellite-based vegetation activity observations, *Biogeosciences*, 10, 4189–4210, doi:10.5194/bg-10-4189-2013, 2013.
- 10 Dee, D. P., Uppala, S. M., Simmons, A. J., Berrisford, P., Poli, P., Kobayashi, S., Andrae, U., Balmaseda, M. A., Balsamo, G., Bauer, P., Bechtold, P., Beljaars, A. C. M., van de Berg, L., Bidlot, J., Bormann, N., Delsol, C., Dragani, R., Fuentes, M., Geer, A. J., Haimberger, L., Healy, S. B., Hersbach, H., Hólm, E. V., Isaksen, I., Kållberg, P., Köhler, M., Matricardi, M., McNally, A. P., Monge-Sanz, B. M., Morcrette, J.-J., Park, B.-K., Peubey, C., de Rosnay, P., Tavolato, C., Thépaut, J.-N., and Vitart, F.: The ERA-Interim reanalysis: configuration and performance of the data assimilation system, *Q. J. Roy. Meteor. Soc.*, 137, 553–597, 2011.
- 15 Defries, R. S., Houghton, R. A., Hansen, M. C., Field, C. B., Skole, D., and Townshend, J.: Carbon emissions from tropical deforestation and regrowth based on satellite observations from the 1980s and 1990s, *P. Natl. Acad. Sci. USA*, 99, 14256–14261, 2002.
- 20 Denman, K., Brasseur, G., Chidthaisong, A., Ciais, P., Cox, P. M., Dickinson, R. E., Hauglustaine, D., Heinze, C., Holland, E., Jacob, D., Lohmann, U., Ramachandran, S., da Silva Dias, P. L., Wofsy, S. C., and Zhang, X.: Couplings Between Changes in the Climate System and Biogeochemistry, in: IPCC, *Climate Change 2007: The Physical Science Basis, Contribution of Working Group I to the Fourth Assessment Report of the Intergovernmental Panel on Climate Change*, edited by: Solomon, S., Qin, D., Manning, M., Chen, Z., Marquis, M., Averyt, K., Tignor, M., and Miller, H., Cambridge University Press, Cambridge, United Kingdom and United States, 2007.
- 25 Dentener, F., Stevenson, D., Ellingsen, K., van Noije, T., Schultz, M., Amann, M., Atherton, C., Bell, N., Bergmann, D., Bey, I., Bouwman, L., Butler, T., Cofala, J., Collins, B., Drevet, J., Doherty, R., Eickhout, B., Eskes, H., Fiore, A., Gauss, M., Hauglustaine, D., Horowitz, L., Isaksen, I. S. A., Josse, B., Lawrence, M., Krol, M., Lamarque, J. F., Montanaro, V., Müller, J. F., Peuch, V. H., Pitari, G., Pyle, J., Rast, S., Rodriguez, J., Sanderson, M., Savage, N. H., Shindell, D., Strahan, S., Szopa, S., Sudo, K., Van Dingenen, R., Wild, O., and Zeng, G.:

20153

- The 5 global atmospheric environment for the next generation, *Environ. Sci. Technol.*, 40, 3586–3594, doi:10.1021/es0523845, 2006.
- Doney, S. C., Lima, I., Feely, R. A., Glover, D. M., Lindsay, K., Mahowald, N., Moore, J. K., and Wanninkhof, R.: Mechanisms governing interannual variability in upper-ocean inorganic carbon system and air–sea CO₂ fluxes: physical climate and atmospheric dust, *Deep-Sea Res. Pt. II*, 56, 640–655, 2009a.
- 5 Doney, S. C., Lima, I., Moore, J. K., Lindsay, K., Behrenfeld, M. J., Westberry, T. K., Mahowald, N., Glover, D. M., and Takahashi, T.: Skill metrics for confronting global upper ocean ecosystem-biogeochemistry models against field and remote sensing data, *J. Mar. Syst.*, 76, 95–112, 2009b.
- 10 Falkowski, P. G., Ziemann, D., Kolber, Z., and Bienfang, P. K.: Role of eddy pumping in enhancing primary production in the ocean, *Nature*, 352, 55–58, 1991.
- Fan, S., Gloor, M., Mahlman, J., Pacala, S., Sarmiento, J., Takahashi, T., and Tans, P.: A large terrestrial carbon sink in North America implied by atmospheric and oceanic carbon dioxide data and models, *Science*, 282, 442–446, 1998.
- 15 Fay, A. R. and McKinley, G. A.: Global trends in surface ocean pCO₂ from in situ data, *Global Biogeochem. Cy.*, 27, 541–557, doi:10.1002/gbc.20051, 2013.
- Friedlingstein, P., Houghton, R. A., Marland, G., Hackler, J., Boden, T. A., Conway, T. J., Canadell, J. G., Raupach, M. R., Ciais, P., and Le Quere, C.: Update on CO₂ emissions, *Nat. Geosci.*, 3, 811–812, 2011.
- 20 Galbraith, D., Levy, P. E., Sitch, S., Huntingford, C., Cox, P., Williams, M., and Meir, P.: Multiple mechanisms of Amazonian Forest biomass losses in three Dynamic Global Vegetation Models under climate change, *New Phytol.*, 187, 647–665, 2010.
- Gedney, N., Cox, P. M., Betts, R. A., Boucher, O., Huntingford, C., and Stott, P. A.: Detection of a direct carbon dioxide effect in continental river runoff records, *Nature*, 439, 835–838, 2006.
- 25 Gent, P. R. and Danabasoglu, G.: Response to increasing Southern Hemisphere winds in CCSM4, *J. Climate*, 24, 4992–4998, 2011.
- Graven, H. D., Gruber, N., Key, R., Khatiwala, S., and Giraud, X.: Changing controls on oceanic radiocarbon: new insights on shallow-to-deep ocean exchange and anthropogenic CO₂ uptake, *J. Geophys. Res.*, 117, C10005, doi:10.1029/2012JC008074, 2012.
- 30 Gruber, N.: Warming up, turning sour, losing breath: ocean biogeochemistry under global change, *Phil. Trans. R. Soc. A*, 369, 1980–1996, doi:10.1098/rsta.2011.0003, 2011.

20154

- Gruber, N., Gloor, M., Mikaloff Fletcher, S. E., Doney, S. C., Dutkiewicz, S., Follows, M. J., Gerber, M., Jacobson, A. R., Joos, F., Lindsay, K., Menemenlis, D., Mouchet, A., Müller, S. A., Sarmiento, J. L., and Takahashi, T.: Oceanic sources, sinks, and transport of atmospheric CO₂, *Global Biogeochem. Cy.*, 23, GB1005, doi:10.1029/2008GB003349, 2009.
- 5 Gruber, N., Lachkar, Z., Frenzel, H., Marchesiello, P., Munnich, M., McWilliams, J., Nagai, T., and Plattner, G.-K.: Eddy-induced reduction of biological production in Eastern Boundary Upwelling Systems, *Nat. Geosci.*, 4, 787–792, doi:10.1038/ngeo1273, 2011.
- Guan, D., Liu, Z., Geng, Y., Lindner, S., and Hubacek, K.: The gigatonne gap in China's carbon dioxide inventories, *Nature Climate Change*, 2, 672–675 doi:10.1038/nclimate1560, 2012.
- 10 Houghton, R. A.: How well do we know the flux of CO₂ from land-use change?, *Tellus B*, 62, 337–351, doi:10.1111/j.1600-0889.2010.00473.x, 2010.
- Hicke, J. A.: NCEP and GISS solar radiation data sets available for ecosystem modeling: description, differences, and impacts on net primary production, *Global Biogeochem. Cy.*, 19, GB2006, doi:10.1029/2004GB002391, 2005.
- 15 Hickler, T., Prentice, I. C., Smith, B., Sykes, M. T., and Zaehle, S.: Implementing plant hydraulic architecture within the LPJ Dynamic Global Vegetation Model, *Global Ecol. Biogeogr.*, 15, 567–577, 2006.
- Huntingford, C., Stott, P. A., Allen, M. R., and Lambert, F. H.: Incorporating model uncertainty into attribution of observed temperature change, *Geophys. Res. Lett.*, 33, L05710, doi:10.1029/2005GL024831, 2006.
- 20 Jain, A. K. and Yang, X.: Modeling the effects of two different land cover change data sets on the carbon stocks of plants and soils in concert with CO₂ and climate change, *Global Biogeochem. Cy.*, 19, GB2015, doi:10.1029/2004GB002349, 2005.
- Janssens, I. A., Freibauer, A., Ciais, P., Smith, P., Nabuurs, G.-J., Folberth, G., Schlamadinger, B., Hutjes, R. W. A., Ceulemans, R., Schulze, E.-D., Valentini, R., and Dolman, A. J.: Europe's terrestrial biosphere absorbs 7 to 12 % of European anthropogenic CO₂ emissions, *Science*, 300, 1538–1542, 2003.
- 25 Jeansson, E., Olsen, A., Eldevik, T., Skjelvan, I., Omar, A. M., Lauvset, S. K., Nilsen, J. E. Ø., Bellerby, R. G. J., Johannessen, T., and Falck, E.: The Nordic Seas carbon budget: sources, sinks, and uncertainties, *Global Biogeochem. Cy.*, 25, GB4010, doi:10.1029/2010GB003961, 2011.
- 30

20155

- Jönsson, A. M., Schröder, M., Lagergren, F., Anderbrandt, O. and Smith, B.: Guess the impact of *Ips typographus* – an ecosystem modelling approach for simulating spruce bark beetle outbreaks, *Agr. Forest Meteorol.*, 166–167, 188–200, 2012.
- Jung, M., Vetter, M., Herold, M., Churkina, G., Reichstein, M., Zaehle, S., Ciais, P., Viovy, N., Bondeau, A., Chen, Y., Trusilova, K., Feser, F., and Heimann, M.: Uncertainties of modeling gross primary productivity over Europe: a systematic study on the effects of using different drivers and terrestrial biosphere models, *Global Biogeochem. Cy.*, 21, GB4021, doi:10.1029/2006GB002915, 2007.
- 5 Kalnay, E., Kanamitsu, M., Kistler, R., Collins, W., Deaven, D., Gandin, L., Iredell, M., Saha, S., White, G., Woollen, J., Zhu, Y., Leetmaa, A., Reynolds, R., Chelliah, M., Ebisuzaki, W., Higgins, W., Janowiak, J., Mo, K. C., Ropelewski, C., Wang, J., Jenne, R., and Joseph, D.: The NCEP/NCAR 40-year reanalysis project, *B. Am. Meteorol. Soc.*, 77, 437–471, 1996.
- Kattge, J., Díaz, S., Lavorel, S., Prentice, I. C., et al.: TRY – a global database of plant traits, *Glob. Change Biol.*, 17, 2905–2935, 2011.
- 15 Khatiwala, S., Tanhua, T., Mikaloff Fletcher, S., Gerber, M., Doney, S. C., Graven, H. D., Gruber, N., McKinley, G. A., Murata, A., Ríos, A. F., Sabine, C. L., and Sarmiento, J. L.: Global ocean storage of anthropogenic carbon, *Biogeosciences Discuss.*, 9, 8931–8988, doi:10.5194/bgd-9-8931-2012, 2012.
- Keeling, C. D. and Whorf, T. P.: Atmospheric CO₂ records from sites in the SIO sampling network, In *Trends: A compendium of data on global change*, Carbon Dioxide Information Analysis Center, Oak Ridge National Laboratory, US Department of Energy, Oak Ridge, Tenn., USA, 2005.
- 20 Keeling, C. D., Bacastow, R. B., Bainbridge, A. E., Ekdahl Jr, C. A., Guenther, P. R., Waterman, L. S., and Chin, J. F. S.: Atmospheric carbon dioxide variations at Mauna Loa observatory, Hawaii, *Tellus*, 28, 538–551, 1976.
- Keeling, C. D., Whorf, T. P., Wahlen, M., and van der Plicht, J.: Interannual extremes in the rate of rise of atmospheric carbon dioxide since 1980, *Nature*, 375, 666–670, 1995.
- Keenan, T., García, R., Friend, A. D., Zaehle, S., Gracia, C., and Sabate, S.: Improved understanding of drought controls on seasonal variation in Mediterranean forest canopy CO₂ and water fluxes through combined in situ measurements and ecosystem modelling, *Biogeosciences*, 6, 1423–1444, doi:10.5194/bg-6-1423-2009, 2009.
- 30 Krinner, G., Viovy, N., and de Noblet-Ducoudré, N., Ogée, J., Polcher, J., Friedlingstein, P., Ciais, P., Sitch, S., and Prentice, I. C.: A dynamic global vegetation model for stud-

20156

- McNeil, B. I. and Matear, R. J.: The non-steady state oceanic CO₂ signal: its importance, magnitude and a novel way to detect it, *Biogeosciences*, 10, 2219–2228, doi:10.5194/bg-10-2219-2013, 2013.
- 5 McKinley, G. A., Takahashi, T., Buitenhuis, E., Chai, F., Christian, J. R., Doney, S. C., Jiang, M.-S., Lindsay, K., Moore, J. K., Le Quéré, C., Lima, I., Murtugudde, R., Shi, L., and Wetzel, P.: North Pacific carbon cycle response to climate variability on seasonal to decadal timescales, *J. Geophys. Res.*, 111, 1–22, 2006.
- 10 McKinley, G. A., Fay, A. R., Takahashi, T., and Metzl, N.: Convergence of atmospheric and North Atlantic carbon dioxide trends on multidecadal timescales, *Nat. Geosci.*, 4, 606–610, 2011.
- Mercado, L. M., Bellouin, N., Sitch, S., Boucher, O., Huntingford, C., and Cox, P. M.: Impact of changes in diffuse radiation on the global land carbon sink, *Nature*, 458, 1014–1017, doi:10.1038/nature07949, 2009.
- 15 Mikaloff Fletcher, S. E., Gruber, N., Jacobson, A. R., Doney, S. C., Dutkiewicz, S., Gerber, M., Follows, M., Joos, F., Lindsay, K., Menemenlis, D., Mouchet, A., Müller, S. A., and Sarmiento, J. L.: Inverse estimates of anthropogenic CO₂ uptake, transport, and storage by the ocean, *Global Biogeochem. Cy.*, 20, GB2002, doi:10.1029/2005GB002530, 2006.
- 20 Myneni, R. B., Keeling, C. D., Tucker, C. J., Asrar, G., and Nemani, R. R.: Increased plant growth in the northern high latitudes from 1981 to 1991, *Nature*, 386, 698–702, doi:10.1038/386698a0, 1997.
- Nemani, R. R., Keeling, C. D., Hashimoto, H., Jolly, W. M., Piper, S. C., Tucker, C. J., Myneni, R. B., and Running, S. W.: Climate-driven increases in global terrestrial net primary production from 1982 to 1999, *Science*, 300, 1560–1563, 2003.
- 25 New, M. G., Hulme, M., and Jones, P. D.: Representing twentieth-century space-climate variability, Part II, Development of 1901–1996 monthly grids of terrestrial surface climate, *J. Climate*, 13, 2217–2238, 2000.
- Norby, R. J., DeLucia, E. H., Gielen, B., Calfapietra, C., Giardina, C. P., King, J. S., Ledford, J., McCarthy, H. R., Moore, D. J. P., Ceulemans, R., De Angelis, P., Finzi, A. C., Karnosky, D. F., Kubiske, M. E., Lukac, M., Pregitzer, K. S., Scarascia-Mugnozza, G. E., Schlesinger, W. H., and Oren, R.: Forest response to elevated CO₂ is conserved across a broad range of productivity, *P. Natl. Acad. Sci. USA*, 102, 18052–18056, 2005.

20159

- Norby, R. J., Warren, J. M., Iversen, C. M., Medlyn, B. E., and McMurtrie, R. E.: CO₂ enhancement of forest productivity constrained by limited nitrogen availability, *P. Natl. Acad. Sci. USA*, 107, 19368–19373, 2010.
- 5 Oleson, K. W., Lawrence, D. M., Bonan, G. B., Flanner, M. G., Kluzek, E., Lawrence, P. J., Levis, S., Swenson, S. C., Thornton, P. E., Dai, A., Decker, M., Dickinson, R., Feddema, J., Heald, C. L., Hoffman, F., Lamarque, J.-F., Mahowald, N., Niu, G.-Y., Qian, T., Randerson, J., Running, S., Sakaguchi, K., Slater, A., Stockli, R., Wang, A., Yang, Z.-L., Zeng, X., and Zeng, X.: Technical description of version 4.0 of the Community Land Model (CLM), NCAR Technical Note NCAR/TN-478+STR, 257 pp., 2010.
- 10 Olivier, J. G. J., Janssens-Maenhout, G., and Peters, J. A. H. W.: Trends in global CO₂ emissions, 2012 report, Background Studies, PBL Netherlands Environmental Assessment Agency, 40 pp., 2012.
- 15 Pacala, S. W., Hurtt, G. C., Baker, D., Peylin, P., Houghton, R. A., Birdsey, R. A., Heath, L., Sundquist, E. T., Stallard, R. F., Ciais, P., Moorcroft, P., Caspersen, J. P., Shevliakova, E., Moore, B., Kohlmaier, G., Holland, E., Gloor, M., Harmon, M. E., Fan, S.-M., Sarmiento, J. L., Goodale, C. L., Schimel, D., and Field, C. B.: Consistent land- and atmosphere-based US carbon sink estimates, *Science*, 292, 2316–2320, 2001.
- 20 Pan, Y., Birdsey, R. A., Fang, J., Houghton, R., Kauppi, P. E., Kurz, W. A., Phillips, O. L., Shvidenko, A., Lewis, S. L., Canadell, J. G., Ciais, P., Jackson, R. B., Pacala, S., McGuire, A. D., Piao, S., Rautiainen, A., Sitch, S., Hayes, D., and Watson, C.: A large and persistent carbon sink in the World's forests, 1990–2007, *Science*, 333, 6045, doi:10.1126/science.1201609, 2011.
- Phillips, O. L., Malhi, Y., Higuchi, N., Laurance, W. F., Núñez, P. V., Vásquez, R. M., Laurance, S. G., Ferreira, L. V., Stern, M., Brown, S., and Grace, J.: Changes in the carbon balance of tropical forests: evidence from long-term plots, *Science*, 282, 439–442, 1998.
- 25 Piao, S. L., Friedlingstein, P., Ciais, P., Zhou, L. M., and Chen, A. P.: Effect of climate and CO₂ changes on the greening of the Northern Hemisphere over the past two decades, *Geophys. Res. Lett.*, 33, L23402, doi:10.1029/2006GL028205, 2006.
- 30 Piao, S., Friedlingstein, P., Ciais, P., Viovy, N., and Demarty, J.: Growing season extension and its impact on terrestrial carbon cycle in the Northern Hemisphere over the past 2 decades, *Global Biogeochem. Cy.*, 21, GB3018, doi:10.1029/2006GB002888, 2007.
- Piao, S. L., Fang, J. Y., Ciais, P., Peylin, P., Huang, Y., Sitch, S., and Wang, T.: The carbon balance of terrestrial ecosystems in China, *Nature*, 458, 1009–1014, 2009a.

20160

- backs using 5 Dynamic Global Vegetation Models (DGVMs), *Glob. Change Biol.*, 14, 1–25, doi:10.1111/j.1365-2486.2008.01626.x, 2008.
- Smith, B., Prentice, I. C., and Sykes, M. T.: Representation of vegetation dynamics in the modelling of terrestrial ecosystems: comparing two contrasting approaches within European climate space, *Global Ecol. Biogeogr.*, 10, 621–637, 2001.
- Stephens, B. B., Gurney, K. R., Tans, P. P., Sweeney, C., Peters, W., Bruhwiler, L., Ciais, P., Ramonet, M., Bousquet, P., Nakazawa, T., Aoki, S., Machida, T., Inoue, G., Vinnichenko, N., Lloyd, J., Jordan, A., Heimann, M., Shibistova, Langenfelds, R. L., Steele, L. P., Francey, R. J., and Denning, A. S.: Weak northern and strong tropical land carbon uptake from vertical profiles of atmospheric CO₂, *Science*, 316, 1732–1735, 2007.
- Sweeney, C., Gloor, E., Jacobson, A. R., Key, R. M., McKinley, G., Sarmiento, J. L., and Wanninkhof, R.: Constraining global air–sea gas exchange for CO₂ with recent bomb ¹⁴C measurements, *Global Biogeochem. Cy.*, 21, GB2015, doi:10.1029/2006GB002784, 2007.
- Tans, P. P., Fung, I. Y., and Takahashi, T.: Observational constraints on the global atmospheric CO₂ budget, *Science*, 247, 1431–1439, doi:10.1126/science.247.4949.1431, 1990.
- Thornton, P. E. and Rosenbloom, N. A.: Ecosystem model spin-up: estimating steady state conditions in a coupled terrestrial carbon and nitrogen cycle model, *Ecol. Model.*, 189, 25–48, 2005.
- Thornton, P. E., Lamarque, J. F., Rosenbloom, N. A., and Mahowald, N. M.: Influence of carbon-nitrogen cycle coupling on land model response to CO₂ fertilization and climate variability, *Global Biogeochem. Cy.*, 21, GB4018, doi:10.1029/2006GB002868, 2007.
- Thornton, P. E., Doney, S. C., Lindsay, K., Moore, J. K., Mahowald, N., Randerson, J. T., Fung, I., Lamarque, J.-F., Feddes, J. J., and Lee, Y.-H.: Carbon-nitrogen interactions regulate climate-carbon cycle feedbacks: results from an atmosphere-ocean general circulation model, *Biogeosciences*, 6, 2099–2120, doi:10.5194/bg-6-2099-2009, 2009.
- Tjiputra, J. F., Assmann, K., and Heinze, C.: Anthropogenic carbon dynamics in the changing ocean, *Ocean Sci.*, 6, 605–614, doi:10.5194/os-6-605-2010, 2010.
- Tucker, C. J., Slayback, D. A., Pinzon, J. E., Los, S. O., Myneni, R. B. and Taylor, M. G.: Higher northern latitude normalized difference vegetation index and growing season trends from 1982 to 1999, *Int. J. Biometeorol.*, 45, 184–190, 2001.
- Van der Molen, M. K., Dolman, A. J., Ciais, P., Eglin, T., Gobron, N., Law, B. E., Meir, P., Peters, W., Phillips, O. L., Reichstein, M., Chen, T., Dekker, S. C., Doubková, M., Friedl, M. A., Jung, M., van den Hurk, B. J. J. M., de Jeu, R. A. M., Kruijt, B., Ohta, T., Rebel, K. T.,

20163

- Plummer, S., Seneviratne, S. I., Sitch, S., Teuling, A. J., van der Werf, G. R., and Wang, G.: Drought and ecosystem carbon cycling, *Agr. Forest Meteorol.*, 151, 765–773, doi:10.1016/j.agrformet.2011.01.018, 2011.
- Vitousek, P. M. and Howarth, R. W.: Nitrogen limitation on land and in the sea: how can it occur?, *Biogeochemistry*, 13, 87–115, 1991.
- Wanninkhof, R.: Relationship between wind speed and gas exchange over the ocean, *J. Geophys. Res.*, 97, 7373–7382, 1992.
- Wanninkhof, R., Park, G.-H., Takahashi, T., Sweeney, C., Feely, R., Nojiri, Y., Gruber, N., Doney, S. C., McKinley, G. A., Lenton, A., Le Quééré, C., Heinze, C., Schwinger, J., Graven, H., and Khatiwala, S.: Global ocean carbon uptake: magnitude, variability and trends, *Biogeosciences*, 10, 1983–2000, doi:10.5194/bg-10-1983-2013, 2013.
- Woodward, F. I. and Lomas, M. R.: Vegetation-dynamics – simulating responses to climate change, *Biolog. Rev.*, 79, 643–670, 2004.
- Woodward, F. I., Smith, T. M., and Emanuel, W. R.: A global land primary productivity and phytogeography model, *Global Biogeochem. Cy.*, 9, 471–490, 1995.
- Zaehle, S. and Dalmonch, D.: Carbon–nitrogen interactions on land at global scales: current understanding in modeling climate biosphere feedbacks, *Curr. Op. Environ. Sustain.*, 3, 311–320, 2011.
- Zaehle, S. and Friend, A. D.: Carbon and nitrogen cycle dynamics in the O-CN land surface model, I: Model description, site-scale evaluation and sensitivity to parameter estimates, *Global Biogeochem. Cy.*, 24, GB1005, doi:10.1029/2009GB003521, 2010.
- Zaehle, S., Medlyn, B. E., De Kauwe, M. G., Walker, A. P., Dietze, M. C., Hickler, T., Luo, Y., Wang, Y.-P., El-Masri, B., Thornton, P., Jain, A., Wang, S., Warlind, D., Weng, E., Parton, W., Iversen, C. M., Gallet-Budynek, A., McCarthy, H., Finzi, A., Hanson, P. J., Prentice, I. C., Oren, R., and Norby, R. J.: Evaluation of eleven terrestrial carbon-nitrogen cycle models against observations from two temperate Free-Air CO₂ Enrichment Studies, *New Phytol.*, submitted, 2013.
- Zhang, X. B., Zwiers, F. W., Hegerl, G. C., Lambert, F. H., Gillett, N. P., Solomon, S., Stott, P. A., and Nozawa, T.: Detection of human influence on twentieth-century precipitation trends, *Nature*, 448, 461–465, doi:10.1038/nature06025, 2007.
- Zeng, N.: Glacial-interglacial atmospheric CO₂ change – the glacial burial hypothesis, *Adv. Atmos. Sci.*, 20, 677–673, 2003.

20164

20165

Table 1. Characteristics of the 9 Dynamic Global Vegetation Models.

Model Name	Abbreviation	Spatial resolution	Land Surface Model	Full Nitrogen Cycle	River Export Flux	Fire simulation	Harvest/ grazing flux	Source
Community Land Model 4CN	CLM4CN	0.5° × 0.5°	Yes	Yes	No	Yes	No	Oleson et al. (2010); Lawrence et al. (2011)
Hyland	HYL	3.75° × 2.5°	No	No	No	No	Yes	Friend et al. (1997); Levy et al. (2004)
Lund-Potsdam-Jena	LPJ	0.5° × 0.5°	No	No	No	Yes	Yes	Sitch et al. (2003)
LPJ-GUESS	LPJ-GUESS	0.5° × 0.5°	No	No	No	Yes	No	Smith et al. (2001)
ORCHIDEE-CN	OCN	3.75° × 2.5°	Yes	Yes	No	No	Yes	Zaehle and Friend (2010); Zaehle et al. (2010)
ORCHIDEE	ORC	0.5° × 0.5°	Yes	No	No	No	No	Krinner et al. (2005)
Sheffield-DGVM	SDGVM	3.75° × 2.5°	No	No	Yes	Yes	No	Woodward et al. (1995)
TRIFFID	TRI	3.75° × 2.5°	Yes	No	No	No	No	Cox (2001)
VEGAS	VEGAS	0.5° × 0.5°	Yes	No	Yes	Yes	Yes	Zeng et al. (2005)

20166

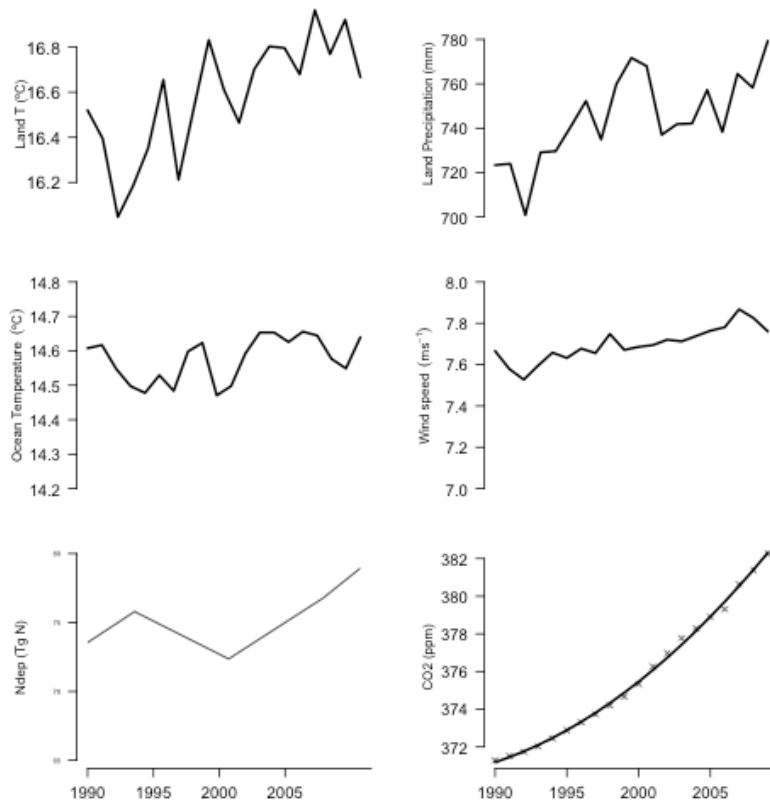


Fig. 2. Global trends in environmental driving variables: Panel 1: temperature; Panel 2: precipitation, Panel 3: atmospheric [CO₂], Panel 4: N deposition.

20169

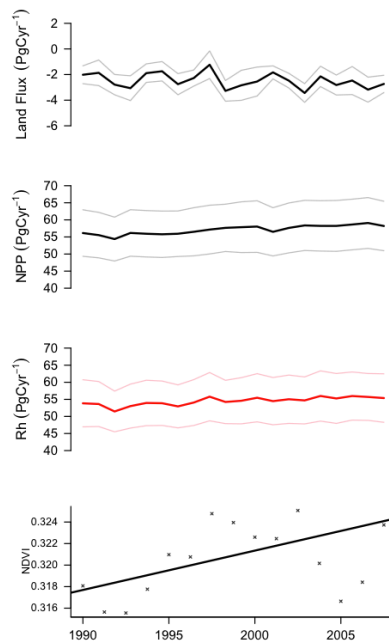


Fig. 3. Global trends in ensemble land model responses. Panel 1: DGVM mean model land sink and standard deviation (grey lines), Component fluxes, NPP (Panel 2), and RH (= RH + wildfire + Riverine C flux) (Panel 3). Remotely sensed trends in annual mean NDVI (crosses), a measure of vegetation greenness, and a linear regression through the data points (bold line) (Panel 4)

20170

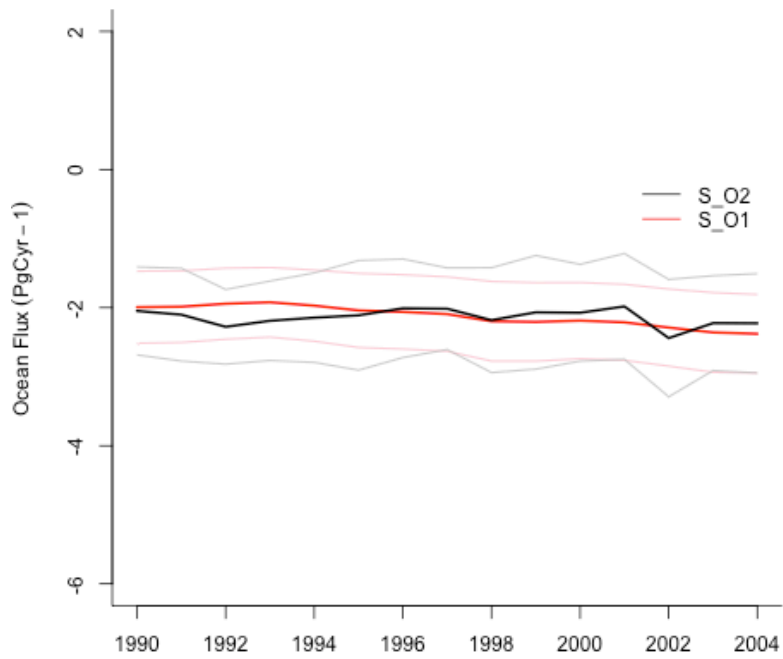


Fig. 4. Global trends in ensemble ocean model fluxes. Black line: results from simulation S_O2 with variable “climate” and increasing CO₂. Red line: results from Simulation S_O1 with constant “climate” and increasing CO₂. The dashed lines indicate the ± uncertainty bands given by the 4 models that contribute to the ensemble mean.

20171

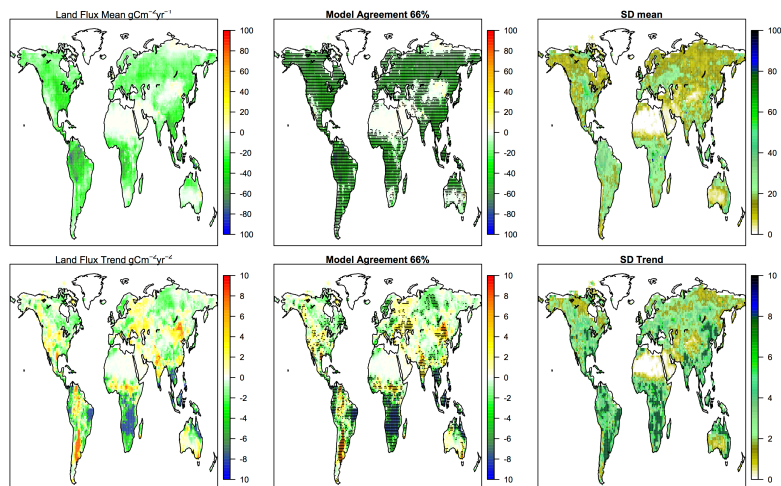


Fig. 5. Gridded maps of average land sink over the period 1990–2009 for the ensemble mean (top left); model agreement with stippling representing agreement for 66% of DGVMs (top middle panel); standard deviation across DGVMs. The bottom left panel shows the trend in land sink across the ensemble, and model agreement; stippling representing agreement of at least 66% of the DGVMs (bottom middle), and the standard deviation of the trend.

20172

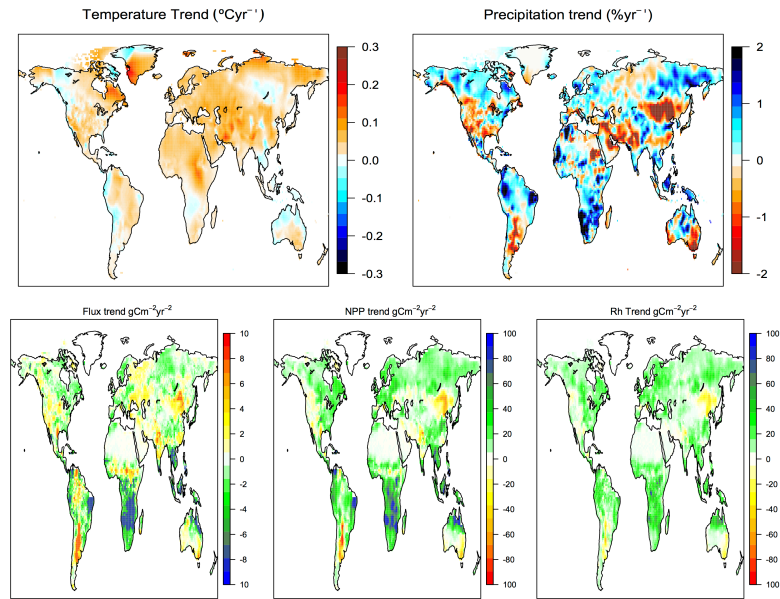


Fig. 6. Multi-panel gridded maps of trends in land climate drivers and process responses. Panel 1: trend in temperature; Panel 2: precipitation; Panel 3: land sink; Panel 4: NPP; Panel 5: Rh (= RH + wildfire + Riverine C flux).

20173

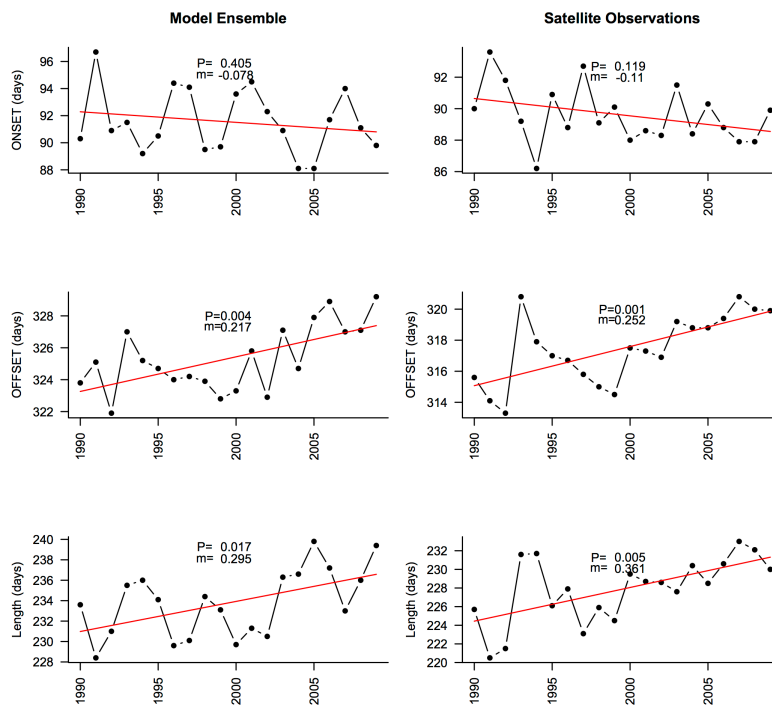


Fig. 7. Ensemble-mean trends in the onset (top), offset (middle) and length of growing season in days for the ensemble mean (left) compared with satellite derived estimates (right).

20174

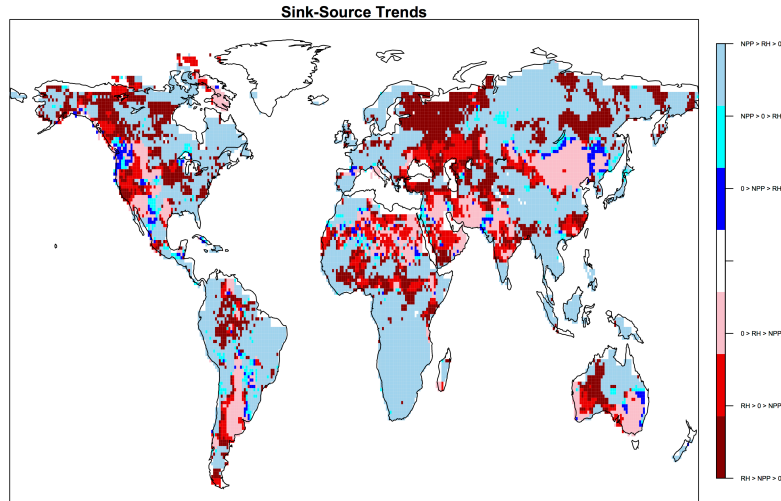


Fig. 8. Qualitative change in processes over the period, 1990–2009. Negative trend in land–atmosphere CO₂ flux: enhanced NPP > enhanced RH (= RH + wildfire + Riverine C flux) (pale blue); enhanced NPP, reduced RH (turquoise); reduced NPP < reduced RH (dark blue). Positive trend in land–atmosphere CO₂ flux: enhanced NPP < enhanced RH (dark red); reduced NPP, enhanced RH (red); reduced NPP > reduced RH (pink).

20175

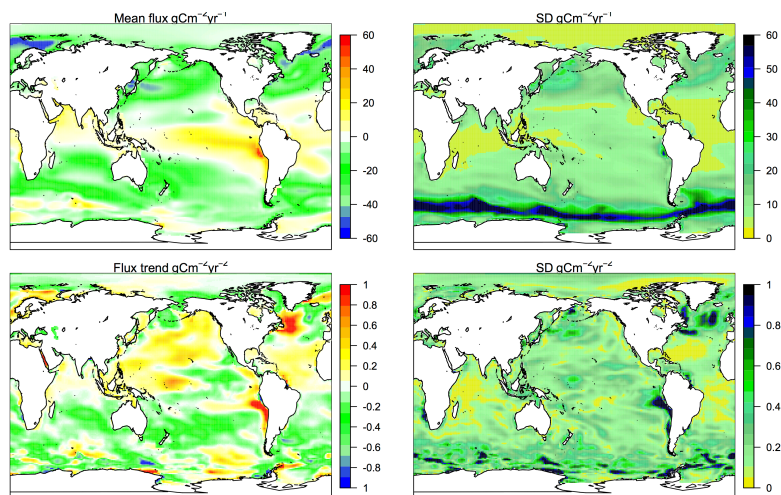


Fig. 9. Gridded maps of the ensemble mean air–sea CO₂ flux over the period 1990–2004 (top left); standard deviation of the mean flux across the four BOGCMs. The bottom left panel shows the trend in the net flux across the ensemble, while the bottom right panel shows the standard deviation of the trend.

20176

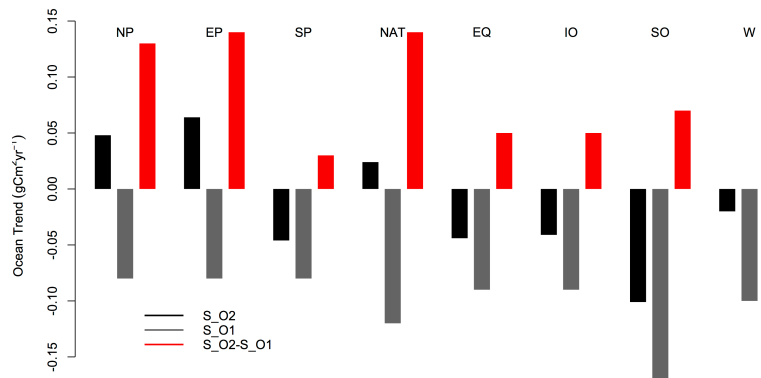


Fig. 10. Regional ocean flux trends from 1990 through 2004 for the standard case, i.e., variable climate and increasing CO₂ (simulation S_O2), and for the constant climate case (simulation S_O1).